LIMNOLOGY
AND
OCEANOGRAPHY

September 2004
Volume 49
Number 5

Limnol. Oceanogr., 49(5), 2004, 1471–1481

Small-scale spatial and temporal variability in coastal benthic O_2 dynamics: Effects of fauna activity

Frank Wenzhöfer[1] *and Ronnie N. Glud*
Marine Biological Laboratory, University of Copenhagen, Strandpromenaden 5, DK-3000 Helsingør, Denmark

Abstract

In situ measurements in a shallow water sediment were performed using three different modules—a microprofiling unit, a transparent benthic chamber, and a planar optode periscope. The combined data set revealed an extremely patchy and variable benthic O_2 distribution primarily due to temporal variations in fauna activity and photosynthesis. A distinct diel pattern in the fauna activity, dominated by *Hediste diversicolor*, resulted in strongly elevated O_2 uptake rates of ~5.3 mmol m^{-2} h^{-1} at the onset of darkness. The activity gradually diminished during the night, and the O_2 uptake decreased to less than half the maximum rate just before sunrise. The volume of oxic sediment around burrow structures was influenced by changing environmental conditions (benthic photosynthesis and fauna activity) but grossly exceeded that below the primary sediment surface. The volume specific respiration rate around burrows was more than seven times higher than the equivalent value at the sediment surface. A budget of the O_2 consumption revealed that the O_2 uptake through the burrow walls just after sunset accounted for the major part of the total O_2 uptake on a diel scale. The study demonstrates that light-driven variations in fauna activity can have great effects on the total benthic O_2 consumption rate with large implications for estimated benthic mineralization rates.

Ignoring minor electron sinks like permanent burial of metal sulfides and the release of dinitrogen, oxygen acts as the ultimate electron acceptor for the benthic degradation of organic material (Canfield et al. 1993). For this reason, benthic oxygen uptake is the most widely used measure of the total sediment mineralization rate (Thamdrup and Canfield 2000). Standard approaches for quantifying benthic O_2 exchange include measurements of O_2 decrease of intact sediment enclosures, either in the laboratory or directly on the seafloor (e.g., Rasmussen and Jørgensen 1992; Smith et al. 1997). Such data provide an overall measure of the total benthic O_2 exchange (TOE) but yield virtually no information on the processes responsible for O_2 consumption or production, the distribution of O_2 within the sediment, or interstitial O_2 dynamics. Measurements of total exchange rates are, therefore, often complemented by microprofile data, which resolve the oxygen distribution within the sediment at a specific point (Archer and Devol 1992; Wenzhöfer and Glud 2002). Steady state O_2 microprofiles unaffected by irrigation allow calculations of the diffusive mediated O_2 exchange (DOE) and the volume specific O_2 consumption or production at any point within the oxic zone (Rasmussen and Jørgensen 1992; Berg et al. 1998). This procedure does, however, represent a one-dimensional approach and assumes that the seafloor is a flat plane. Accounting for the fact that the sediment surface is, in reality, a varied topographic landscape generally increases the calculated DOE of coastal sediments by ~10% (Røy et al. 2002; Glud et al. 2003). Another problem of microsensor-derived data is that they only poorly reflect the horizontal variation in aerobic activity (Fenchel and Glud 2000).

In many coastal sediments, faunal activity greatly influences sediment structure (Solan and Kennedy 2002) and contributes significantly to the benthic O_2 consumption (Aller 1998; Kristensen 2000). The fauna-mediated O_2 uptake rate of marine sediments has generally been calculated from estimates on faunal biomass and laboratory-determined respiration measurements, or from empirical relations between biomass and metabolic rates of various specimens (e.g., Piepenburg et al. 1995). Such estimates do not include irrigation related activity, where the transport of oxygenated water

[1] To whom correspondence should be addressed. Present address: Max-Planck-Institute for Marine Microbiology, Celsiusstrasse 1, 28359 Bremen, Germany (fwenzhoe@mpi-bremen.de).

Acknowledgments

We thank Anni Glud for construction of oxygen electrodes and Lars Rickelt for planar optode manufacture. M. Huettel and another anonymous reviewer are thanked for constructive critiques during the review process, which improved the manuscript. The study was supported by grants from the European Community Marie Curie Fellowships to F.W. (HPMF-CT-2000-00569), the EU project COAS (EVK3-CT-2002-00076), the Danish National Science Research Council (R.G.), and the Carlsberg Foundation (R.G.).

deep into the sediment leads to increased sediment O_2 uptake rates (Forster and Graf 1995). An alternative procedure for quantifying the fauna-related O_2 uptake is simply to subtract the diffusive O_2 uptake from the total O_2 uptake (e.g., Archer and Devol 1992). However, in order to correctly represent the faunal activity, measurements should ideally be done in situ and with relatively large benthic chambers (Devol and Christensen 1993; Glud and Blackburn 2002).

In coastal waters, the activity of benthic microphytes may further complicate matters. The often patchy distribution of benthic microphytes and the temporal variations in light intensity regulate the benthic photosynthesis and consequently the benthic O_2 dynamic, enhancing the availability of O_2 at daytime and diminishing it at night (Glud et al. 2002). Further, the autotrophic activity can stimulate the heterotrophic microbial activity through leakage of photosynthesates (Fenchel and Glud 2000).

The advent of planar optodes for imaging the spatial distribution of O_2 has provided a much more detailed insight into the O_2 dynamics of marine sediments than, for example, traditional one-dimensional microprofile approaches (Glud et al. 1996, 2001; Precht et al. 2004). The technique allows continuous two-dimensional quantification of the O_2 distribution across the sediment–water interface at high spatial ($\sim$100 μm) and temporal resolution (seconds) (Glud et al. 1999).

The present database on in situ O_2 dynamics in natural undisturbed sediments, as well as in situ based estimates on fauna-related O_2 uptake rates, is still very limited (e.g., Archer and Devol 1992; Glud et al. 2003). In the present study we apply microprofiles, benthic chamber incubations and planar optode imaging to resolve, in situ, the O_2 dynamics of a coastal sediment at hitherto unobtainable temporal and spatial scales. The effects of macrofaunal activity on O_2 distribution are quantified and discussed in the context of benthic mineralization.

Materials and methods

Study site—Measurements were performed in September 1998 (microsensor and benthic chamber) and February 2002 (benthic chamber and planar optode) at a shallow water subtidal site just outside our laboratory in Helsingør, Denmark. During measurements, the water depth varied between 0.8 and 1.3 m, and on both occasions patches of diatoms covered the fine-grained sediment. The upper 5 mm of the sediment had an approximate porosity of 0.6 (v/v; determined from density and weight loss drying at 105°C for 24 h), and the organic carbon content was 0.5–1% (determined as loss on ignition after combusting at 450°C for 24 h). Bottom water temperature and oxygen concentration varied between 15–18.5°C and 3–5°C, and 232–244 and 312–356 μmol L^{-1}, while the salinity was around 21 and 29 in September and February, respectively. On both occasions, the in situ instruments were placed adjacent to one another by lowering them from a small floating platform. All instruments measured continuously for 24 h. During incubations, the ambient light levels in air and at the seafloor were continuously recorded by two planar light loggers (HOBO, Onset) intercalibrated toward a LI-192SA underwater quantum sensor (LiCor) connected to a light meter (LiCor LI-1000). For data discussion and budget calculations, the 24-h measuring period was divided into two phases, daytime and nighttime, using the ambient light level as a threshold. Nighttime was defined as the phase when the ambient irradiance was <5 μmol quanta m^{-2} s^{-1} at the sediment surface.

In situ measurements—In September, a profiling module equipped with four Clark-type microelectrodes (Gundersen and Jørgensen 1990) was used to repeatedly measure one-dimensional O_2 microprofiles. The microelectrodes were equipped with an internal reference and a guard cathode (Revsbech 1989). The outer tip diameter of the electrodes was 10–25 μm, and the sensors had a response time <1 s and a stirring sensitivity $<1\%$ (Revsbech 1989; Glud et al. 2000). The microelectrodes had a linear response toward the O_2 concentration and were calibrated in situ using constant readings in bottom water with a known O_2 concentration (determined by Winkler titration) and the anoxic parts of the sediment. After placing the instrument at the sediment surface, the central sensor array was lowered in steps of 50 μm, and all sensor readings were stored internally at each depth horizon. Microprofiles were measured every $\sim$30 min along the same vertical axis for a total period of 24 h.

From most of the obtained microprofiles, the relative position of the sediment surface was identified as a distinct break in the otherwise linear concentration gradient resolved within the diffusive boundary layer (DBL) (Jørgensen and Revsbech 1985). The O_2 penetration depth could be inferred directly from the microprofiles, while the DOE (diffusive oxygen uptake) was calculated by Fick's first law of diffusion (Rassmussen and Jørgensen 1992):

$$\mathrm{DOE} = D_0 \frac{dC}{dz} \tag{1}$$

where D_0 is the molecular diffusion coefficient for O_2 at the given temperature and salinity and C is the oxygen concentration at position z within the DBL. Calculated negative values represent a net diffusive O_2 uptake of the sediment, while positive values indicate a net release of O_2 from the sediment to the overlying water column. Alternatively, for the vertical microprofiles extracted from the two-dimensional images (*see planar optode measurements*), the DOE was calculated from the interstitial O_2 profiles. Thus, the sediment diffusion coefficient D_S was determined from the empirical relationship $D_S = D_0\Phi^{m-1}$, where Φ is the porosity and $m = 2$ (Ullmann and Aller 1982).

Both in February and September, the total benthic O_2 exchange was measured with a modified module based on the benthic chamber lander Elinor (Glud et al. 1995). The module was equipped with a transparent squared Plexiglas chamber (30 × 30 cm) with rounded corners and enclosed a sediment area of 896 cm^2 with a 10 cm overlying water column. During the incubations, a central rotating stirrer created a DBL thickness of approximately 600 μm for most of the enclosed sediment area (Glud et al. 1995), which was comparable to in situ conditions. The O_2 concentration of the enclosed water was continuously monitored with time by two Clark-type minielectrodes mounted in the chamber lid.

The sensors had a reinforced outer casing but had the same measuring characteristics as outlined above (Glud et al. 2000). The sensors were calibrated against bottom water samples and a zero reading recorded on shore at in situ temperature. During the 24-h deployments, the chamber lid was periodically opened for 30 min to exchange the enclosed water with ambient seawater. An online motor, controlled from the floating platform, regulated this procedure. The same sediment area was repeatedly incubated over the 24-h cycles throughout the deployments. Total oxygen uptake (TOE) was calculated from the linear change in O_2 concentration versus time, accounting for the enclosed water volume, which was determined at the end of the incubation (negative values indicate a net total O_2 uptake, and positive values specify a net total O_2 release). Also, at the end of the incubation, the upper 10 cm of the enclosed sediment was recovered and sieved through a 500-μm mesh screen to collect the macrofauna. The fauna was identified, and the wet and dry weight (after 24 h at 70°C) of each species was determined.

In February, the in situ planar optode module (Fig. 1) described by Glud et al. (2001) was deployed along with the benthic chamber. The planar optode module is similar in design with sediment profile imagery (SPI) systems used for in situ studies of the animal–sediment relation (Rhoads and Cande 1971). The planar optode was based on a Ruthenium-fluorophore embedded in plasticized polyvinyl chloride (PVC) sandwiched between a transparent support foil and an optical insulation of black silicon (Glud et al. 1996). This sensor foil was placed on the front of the inverted periscope, and images of the O_2 quenched fluorescence, emitted by the immobilized fluorochrome, were recorded by a digital charge coupled device (CCD) camera (SensiCam, PCO Computer Optics) placed in a central housing (Fig. 1). The camera was equipped with a wide-angle lens (25-mm Nikon) and an excitation filter (long-pass filter OG 570, Schott). The central housing hosted a light source (blue light emitting diodes [LED], $\lambda = 470$ nm, Nichia) with an emission filter (Unaxis C-54, Linos), a dichroic filter (Unaxis O-59, Linos), and associated electronics (Fig. 1). The in situ planar optode module was cross-linked via a fiber-optic cable to a personal computer placed on the floating platform. The entire housing with the inverted periscope was placed in an elevator system fixed to a tripod. The motorized elevator was moved downward, in 1-mm steps, using an electronic controller. For more details on the in situ planar O_2 optode instrument see Glud et al. (2001).

A pixel-by-pixel two-point calibration was performed in situ by placing the sensor foil in the overlying water of known O_2 concentration and in the anoxic sediment. The obtained TIFF (tagged image file format) images were converted into oxygen concentration images by a modified Stern-Volmer equation (Klimant et al. 1995):

$$\frac{I}{I_0} = \frac{\tau}{\tau_0} = \alpha + \frac{1}{(1 + K_{sv}C)}(1 - \alpha) \qquad (2)$$

where I_0 and τ_0 represent the fluorescence intensity and lifetime, respectively, in absence of O_2, and I and τ represent the fluorescence intensity and lifetime, respectively, at an O_2

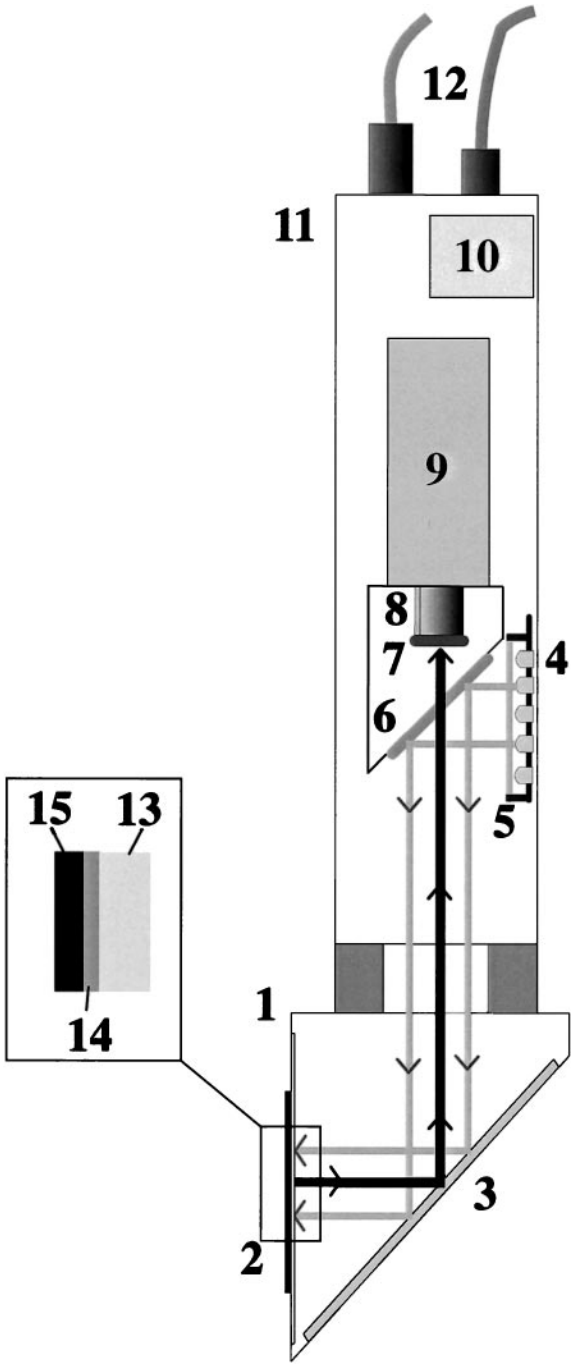

Fig. 1. Schematic drawing of the in situ planar optode module. (1) inverted periscope, (2) planar optode, (3) mirror, (4) LED array, (5) excitation filter, (6) dichroic filter, (7) emission filter, (8) camera lens, (9) CCD camera, (10) electronics controlling the power supply for the LEDs, (11) central underwater housing, (12) cable connections (one electrical for general power supply and one fiber-optic for camera control), (13) support foil (125 μm), (14) fluorescence dye layer (~10 μm), and (15) silicone insulation (~45 μm). Arrows indicate the light paths of the excitation and emission light (modified from Glud et al. 2001).

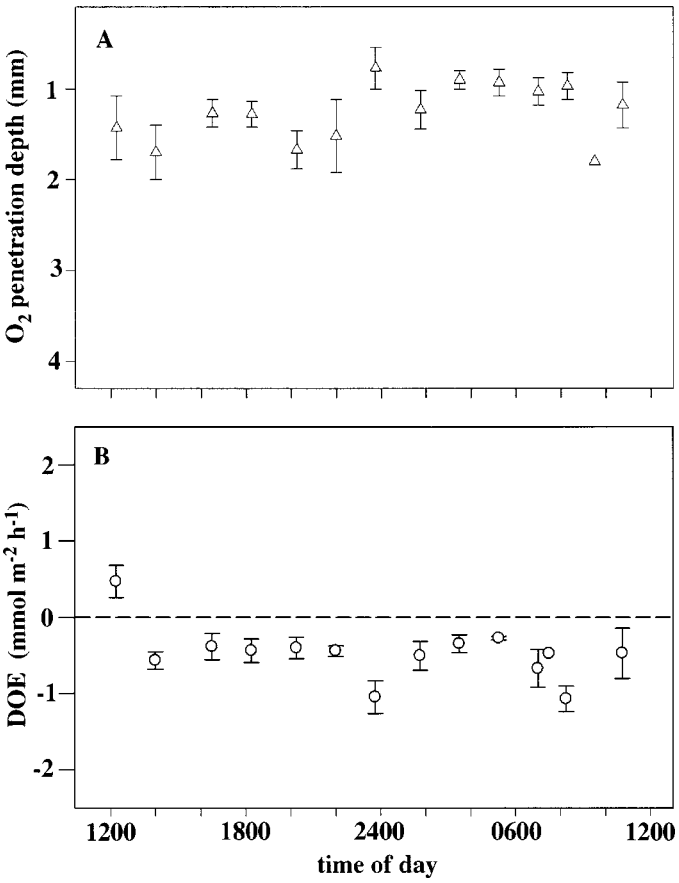

Fig. 2. In situ oxygen dynamic as measured by microelectrodes in September. (A) O_2 penetration depth and (B) diffusive O_2 exchange (DOE) as determined from the microprofiles over a 24-h period.

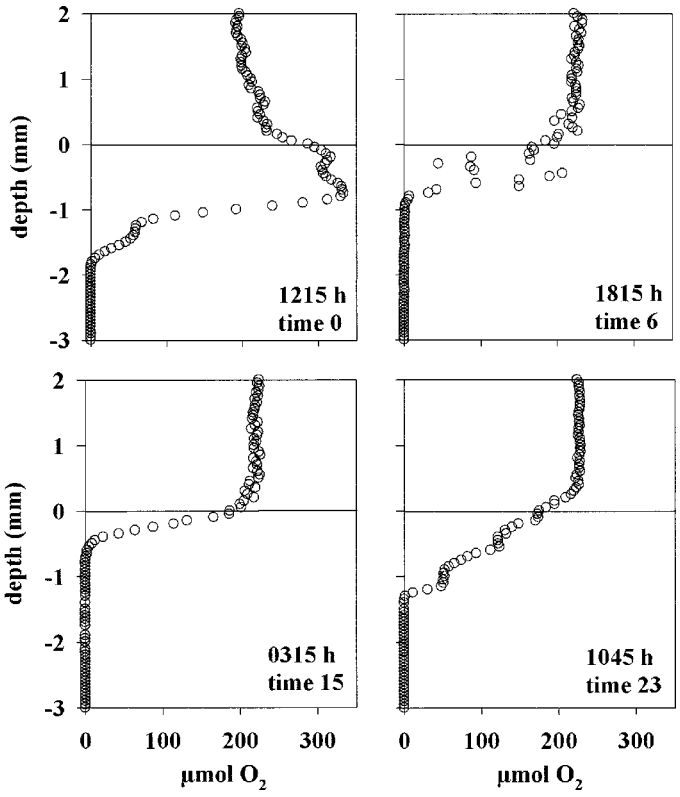

Fig. 3. Example of typical O_2 microprofiles obtained during the measuring campaign in September.

concentration of *C*. K_{sv} is the quenching coefficient of the fluorophore, and α is the nonquenchable fractionation of the emitted fluorescence. In the present study, we used the fluorescent lifetime quantified by the so-called shark-fin approach (Hartmann et al. 1997) as the O_2 sensitive parameter and an image constant $\alpha = 0.15$. After placing the sensor in the sediment, images were recorded every 15 min (except for two short periods at the beginning and around midnight, where the interval was 30 min) for a total period of 24 h. The obtained oxygen images covered an area of 7×5 cm with a spatial pixel resolution of $\sim$105 µm (CCD camera chip size 640×480 pixel). For more details about sensing foils and the measuring routine see Holst et al. (1998) and Glud et al. (1996, 2001).

Results

The high-resolution one-dimensional O_2 microprofiles only expressed a moderate diel variation. In September, the O_2 penetration depth measured with microelectrodes varied between 1.5 and 0.9 mm during a 24-h period with minimum values occurring during darkness (Fig. 2A). The average O_2 penetration depth amounted to 1.23 ± 0.35 mm. During daytime, benthic primary production occasionally resulted in a net export of O_2 from the sediment; however, most profiles reflected a net O_2 uptake (Figs. 2B and 3). Most one-dimensional microprofiles showed a smooth decline in O_2 concentration, but occasional irregularities and O_2 peaks deep down in the sediment indicated benthic fauna driven irrigation (Fig. 3). This was especially apparent in microprofiles obtained just around sunset (1800 h). Some microelectrodes penetrated through fauna burrows, indicating that bottom water with higher O_2 concentration was drawn down into suboxic or anoxic sediment layers (Fig. 3 1815 h). It was, however, difficult to quantify any temporal or spatial pattern in the O_2 dynamics from the four microprofiles obtained simultaneously. Further, the strong faunal activity invalidated many of the DBL determined DOE rates. However, the data showed only a limited variability in the DOE, apart from the occasional net O_2 release during daytime. On average, the DOE measured at nighttime resulted in rates of -0.5 ± 0.3 mmol m^{-2} h^{-1}, while the equivalent daytime value was -0.45 ± 0.4 mmol m^{-2} h^{-1}.

TOE rates, integrating the net exchange across a sediment area of $\sim$900 cm^2, revealed a much more dynamic O_2 exchange during the diel cycle (Fig. 4A,B). At midday, $\sim$200 µmol quanta m^2 s^{-1} reached the sediment surface (Fig. 4C,D), and in September the average TOE during daytime was -1.3 ± 0.5 mmol m^{-2} h^{-1}, while the net exchange in February was $\sim$0, indicating that the benthic community was close to its light compensation point during daytime. However, on both occasions the TOE increased dramatically at sunset and reached maximum values of -5.8 and -4.5

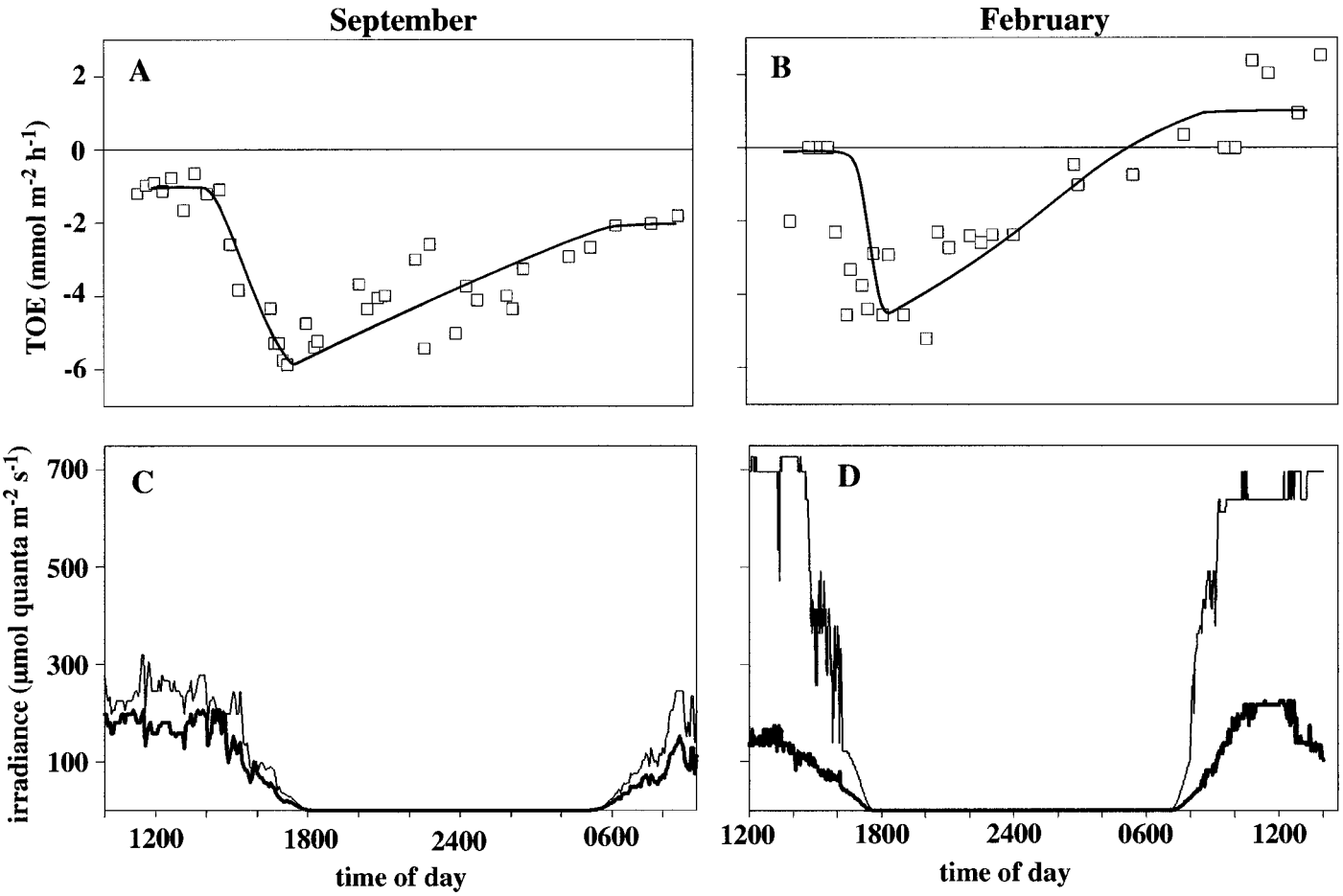

Fig. 4. In situ oxygen dynamic as measured by the benthic chamber in September and February. (A) Total O_2 exchange (TOE) over 24-h periods; lines were hand drawn. (B) Down-welling irradiance in air (light lines) and at the seafloor (bold line) on the two occasions.

mmol m^{-2} h^{-1} in September and February, respectively. The high O_2 consumption rates gradually decrease overnight, reaching a constant rate at sunrise comparable to the values obtained prior to sunset the day before. The average night-integrated (12 h) total O_2 consumption rates were -45.6 and -26.4 mmol m^{-2} in September and February, respectively, while the comparable daytime values were -26.3 and -8.4 mmol m^{-2}. Obviously, the net exchange of O_2 at daytime was affected by the benthic primary production, and in February there was a positive correlation between the total net exchange rates and the ambient light levels during daytime; this pattern was less apparent in September.

The sediment recovered after the deployments solely contained one macrofaunal species, the polychaete *Hediste diversicolor,* with a density of 450 and 600 individuals per square meter in September and February, respectively. The total wet weight was 49.3 and 31.0 g m^{-2}, and the dry weight was 8.6 and 5.7 g m^{-2}. The individual wet weights of single specimen were in the range of 0.14–0.23 g (mean 0.2 g) in September and 0.008–0.06 g (mean 0.05 g) in February.

The initial oxygen images obtained by the planar optode system reflected horizontal isolines with a uniform O_2 penetration depth only disrupted by occasional spots of benthic photosynthesis (Fig. 5A 1300 h). On a diel cycle, the vertical microprofiles extracted from the images at areas visually unaffected by fauna activity revealed an O_2 penetration depth of 5.7 $\pm$ 1.5 mm, which is higher than values obtained by the microelectrodes in September. The DOE rates calculated from extracted profiles were also significantly less when compared to the September values (0.1 mmol m^{-2} h^{-1} in February vs. 0.5 mmol m^{-2} h^{-1} in September). In general, measurements in February showed lower O_2 exchange rates (diffusive and total), which suggests that the deeper O_2 penetration depth was a consequence of higher O_2 concentration in the bottom water and lower microbial activity. The horizontally aligned O_2 isolines during daytime (Fig. 5A 1300 h and Fig. 5B 1700 h) were dramatically changed at sunset when burrow systems became visible because of faunal ventilation (Fig. 5C 1800 h and Fig. 5D 2000 h). Ventilation of existing burrows and, thus, oxygenation of deeper reduced sediment layers must also have taken place during daytime, but the fact that we did not observe this strongly suggests less faunal activity during this period. During night, old burrows were abandoned and new burrows along the planar optode were constructed (Fig. 5). Occasionally water ejected from the fauna inhabiting the burrows formed plumes of anoxic water just above the sediment surface (Fig. 5E 2200 h). The sediment was intensively reworked, and all burrows

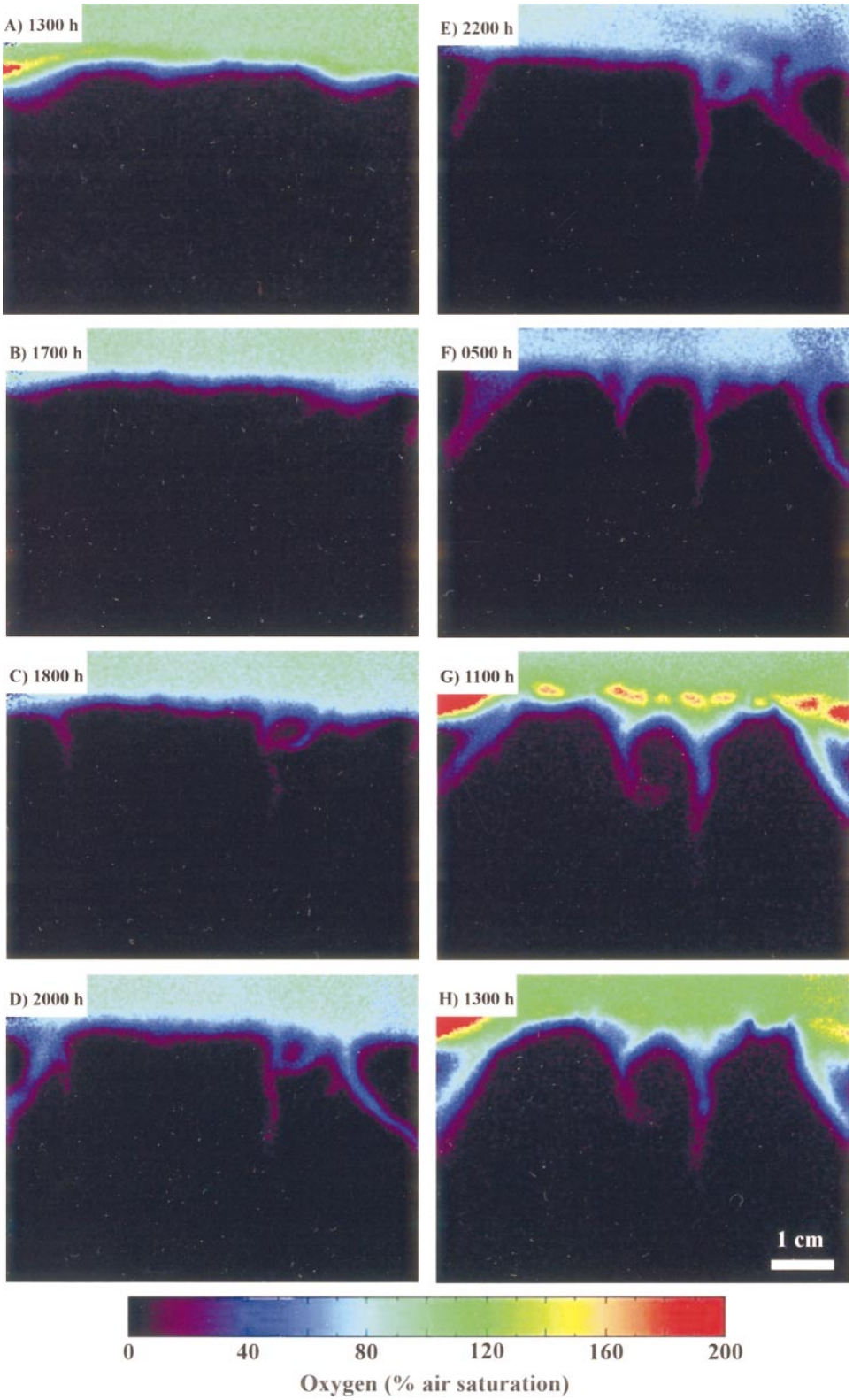

Fig. 5. Selected in situ O_2 images measured during the diel campaign in February. (A) At the beginning (1300 h) of the measurements an almost laminated horizontal structure of the O_2 distribution is evident. (B)–(F) With time, burrow structures appear transporting oxygenated water deeper into the sediment. (E) 2200 h, shows an outburst of anoxic water due to ventilation caused by *Hediste diversicolor*. During daytime (G), 1100 h and (H), 1300 h, hot spots of benthic photosynthesis were apparent enhancing the O_2 concentration at the sediment surface. The complete 24-h sequence of images composed to a movie can be seen in Web Appendix 1, http://www.aslo.org/lo/toc/vol_49/issue_5/1471a1.html.

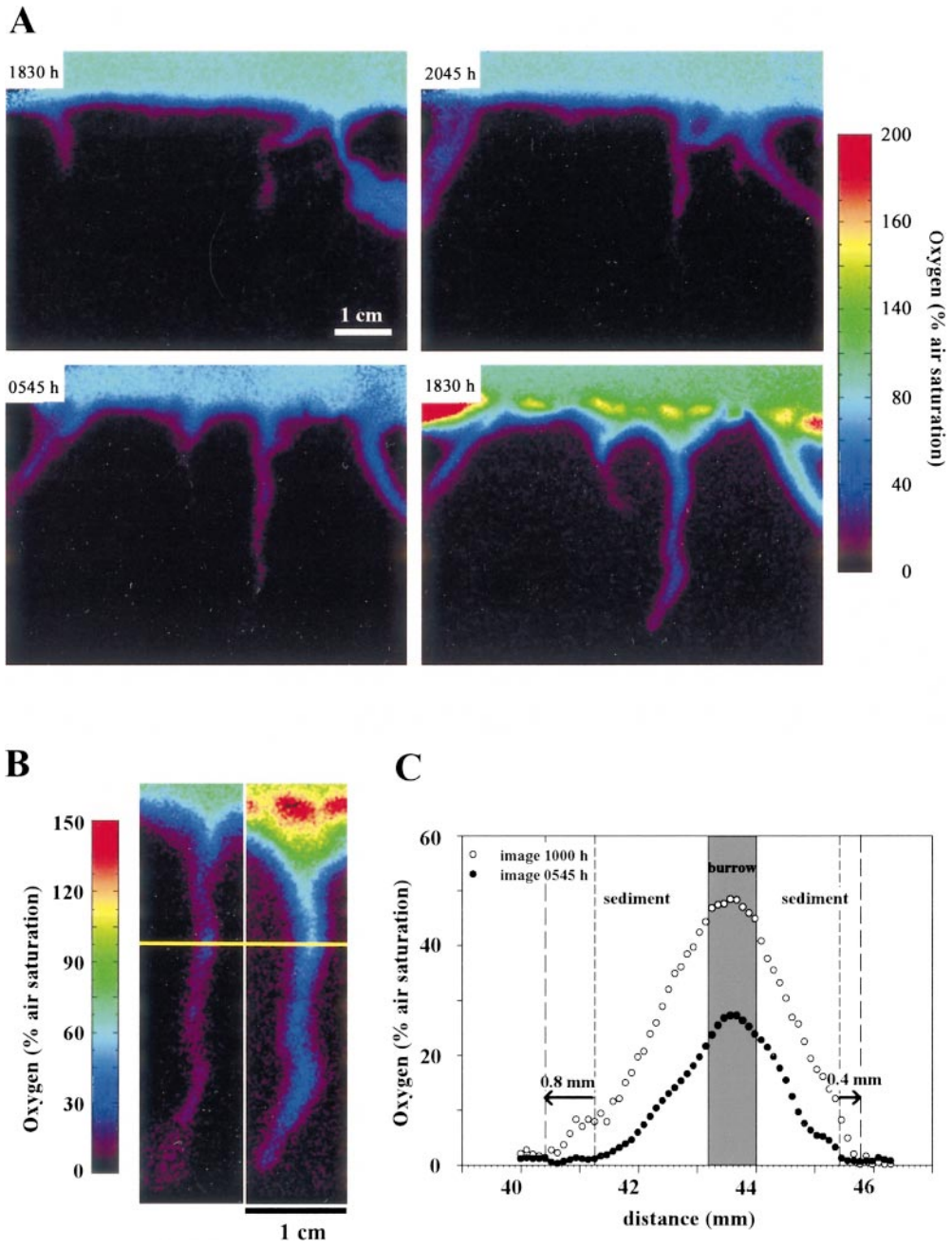

Fig. 6. Examples of the spatial and temporal O_2 distribution in sediments influenced by burrowing fauna and photosynthesis. (A) Two sets of O_2 images (1830–2045 h and 0545–1000 h) showing the highly variable O_2 distribution around animal burrows. (B) Close up of the vertical burrows from image A (0545 h and 1000 h). (C) Horizontal oxygen concentration profiles in and around an animal burrow as extracted from the O_2 images in (B); indicated by the yellow line.

were at some point ventilated leading to a very dynamic O_2 distribution in the upper centimeters of the sediment at nighttime. The bottom water O_2 concentration 1 cm above the sediment surface decreased during the night, but at sunrise benthic primary production increased the O_2 concentration at the sediment surface. Burrows that still were ventilated were now exposed to much higher levels of O_2 as the inhalant water passed the phototrophic community. The irrigating polychaets introduced oxygenated water down to at least 2–3 cm into the sediment (Fig. 5). In the absence of any obvious burrow structure, the O_2 penetration depth of the surrounding sediment was only a few millimeters.

Overall, the two-dimensional oxygen imaging performed in February showed a highly dynamic surficial O_2 distribution that only was poorly resolved by the one-dimensional microprofiles. However, the images supported the results of the total incubation approach showing intensified activity at sunset and during the night. The whole sequence of planar O_2 optode images (81 images), covering a period of 24 h, is combined to a short movie visualizing the benthic oxygen

dynamics (see Web Appendix 1, http://www.aslo.org/lo/toc/vol_49/issue_5/1471a1.html).

Discussion

Diel rhythm in net O_2 exchange rates—The present data demonstrate a variable TOE with a highly elevated O_2 consumption rate at sunset followed by a gradual decrease during the night. This pattern could in principle be caused by two factors: (1) enhanced availability of photosynthesates accumulating during daytime that subsequently become exhausted during nighttime or (2) diel rhythms in faunal activity. Light stimulated respiration in benthic communities is a well-documented fact (e.g., Epping and Jørgensen 1996), and measurements performed at the same site as the present study documented a light-enhanced respiration of at most 60% in diatom covered sediment patches (Fenchel and Glud 2000). The same study also documented a moderate decrease in dark respiration overnight of ~10–15% in sediments deprived of most benthic fauna. This is significantly less than in our present measurements, where the TOE decreased by >60% during the night. However, Fenchel and Glud (2000) used higher light intensities and longer light periods than in the present study, stimulating any photosynthetic-related response. Enhanced heterotrophic activity caused by accumulated labile carbon is, therefore, an unlikely explanation for the observed temporal dynamic in the O_2 consumption rates at night. Further, we did not observe any distinct pattern in the in situ DOE rates. We conclude that the change in the total O_2 consumption rate experienced at nighttime reflected variations in faunal activity. *H. diversicolor* was the only macrofauna at the investigated site and is predated by fish. The dramatic increase in O_2 consumption at sunset matched visual observations on increased faunal activity at the sediment surface. It was observed that many animals left their burrow systems and moved around at the sediments surface just around sunset. The capability of switching between deposit feeding and suspension feeding in *H. diversicolor*, which is triggered by high phytoplankton concentrations, has been described (e.g., Riisgaard and Kamermans 2001). However, low phytoplankton concentrations in spring and autumn and the visible activity of the polychaetes at the sediment surface make this explanation for the elevated TOE unlikely. We speculate that the observed behavior is an attempt to avoid predation during daytime, where the animal would be exposed. Such a diel rhythm of benthic fauna activity has been reported for other marine invertebrates like isopods and ophiuroidae (McLachlan 1983; Rosenberg and Lundberg in press). Rosenberg and Lundberg (in press) relate the enhanced activity of *Amphiura filiformis* during night to a trade-off between feeding efficiency and predator avoidance. However, to our knowledge such a diel activity rhythm for polychaets and a fauna induced diel pattern in TOE has not been previously reported.

In September, the TOE of the investigated sediment as integrated over the entire 24-h period was 71.3 mmol O_2 m^{-2} d^{-1}. This is a very high value compared with measurements performed in comparable shallow water sediments (~50 mmol m^{-2} d^{-1} by Therkildsen and Lomstein 1993; 35–40 mmol m^{-2} d^{-1} by Glud et al. 2003). In September, the diatom cover was low, no net photosynthesis was observed in any of the total incubations, and only very few O_2 microprofiles expressed a positive net photosynthesis (Figs. 2 and 3). Ignoring the small contribution of photosynthesis at daytime, 73% of the daily integrated O_2 consumption took place from sunset to sunrise. *H. diversicolor* is a common infauna specimen in many benthic communities (e.g., Kristensen 2000), but it remains to be shown to what extent other light-exposed populations express a similar diel rhythm. However, in principle similar behavior can be expected in all coastal settings where light reach the sediment surface (i.e., where benthic primary production can be observed) and where *H. diversicolor* make a significant contribution to the benthic community. It can, however, also be speculated that other infauna species potentially express a similar behavior (e.g., Rosenberg and Lundberg in press). If diel rhythms of fauna activities are common, our present database on in situ O_2 net exchange rates in coastal environments may underestimate actual rates, since most measurements are performed during daytime.

Benthic fauna effects on sediment O_2 exchange—The difference between the TOE and DOE obtained simultaneously in sediments with a net O_2 uptake largely quantifies the fauna-mediated O_2 uptake. This includes the fauna respiration and the stimulated microbial consumption following irrigation of otherwise anoxic sediment layers. As benthic photosynthesis during daytime in February added significantly to the benthic O_2 exchange, we have only evaluated the fauna-mediated O_2 uptake in September and nighttime in February in larger detail. In our study, the diel fauna-stimulated O_2 consumption amounted to -57.1 mmol m^{-2} d^{-1}, which equals 80% of the diel integrated total O_2 uptake. On the diel cycle, the ratio between TOE and DOE in September varied between 0.9 and 11. The ratio increased rapidly at sunset from 2 to 11 before it gradually declined overnight, reaching nearly the same ratio of 2–3 just before sunrise the next day. During night (12 h), the fauna-mediated O_2 uptake amounted to -40.5 (or 94% of the total O_2 uptake at night) and -30.3 mmol m^{-2} d^{-1} (or 91% of the total O_2 uptake at night), with a maximum consumption rate of -4.3 and -5 mmol m^{-2} h^{-1} at sunset in September and February, respectively.

The simplified approach of quantifying the DOE from one-dimensional microprofiles does not account for changing any potential impedance of the DBL during the measurements. The average in situ DBL thickness during the September campaign was 0.65 ± 0.07 mm (SD, $n = 42$). This value is probably underestimated because of microsensor compression during the measurements (Glud et al. 1994). However, the DBL thickness created inside the benthic chamber (~0.6 mm, Glud et al. 1995) was close to the measured DBL thickness. A rough estimate on the extent by which the DBL potentially impeded the benthic exchange rate, and thereby to what extent changes might have influenced the O_2 uptake, can be derived from the ratio $C_0 : C_w$, where C_0 is the O_2 concentration at the sediment surface and C_w is the O_2 concentration in the well-mixed bottom water (Jørgensen and Boudreau 2001). $C_0 : C_w$ ratios >0.6 indicate

Table 1. In situ O_2 consumption mass budget for a shallow water sediment inhabited by benthic fauna (*Hediste diversicolor*) at different times during a 24-h cycle. (Negative values indicate an O_2 uptake; values in parentheses represent percentage of the total O_2 exchange; for more explanation *see text*).

	Time of day	Total O_2 exchange (mmol m^{-2} h^{-1})	Diffusive O_2 exchange (mmol m^{-2} h^{-1})	Fauna-mediated O_2 uptake* (mmol m^{-2} h^{-1})	Fauna respiration† (mmol m^{-2} h^{-1})	Burrow O_2 uptake‡ (mmol m^{-2} h^{-1})
February	1845	−2.92 (100%)	−0.25 (8.5%)	−2.67 (91.5%)	−0.2 (6.8%)	−2.47 (84.7%)
nighttime	2300	−2.38 (100%)	−0.18 (7.6%)	−2.20 (92.4%)	−0.2 (8.4%)	−2.00 (84.0%)
	0545	−0.74 (100%)	−0.21 (28.4%)	−0.53 (71.6%)	−0.2 (27.0%)	−0.33 (44.6%)
September	1815	−4.75 (100%)	−0.44 (9.3%)	−4.31 (90.7%)	−0.3 (6.3%)	−4.01 (84.4%)
nighttime	0145	−3.98 (100%)	−0.50 (12.6%)	−3.48 (87.4%)	−0.3 (7.5%)	−3.18 (79.9%)
	0515	−2.65 (100%)	−0.27 (10.2%)	−2.38 (89.8%)	−0.3 (11.3%)	−2.08 (78.5%)
September	1400	−1.21 (100%)	−0.57 (47.1%)	−0.64 (52.9%)	−0.3 (24.8%)	−0.34 (28.1%)
daytime	0815	−2.04 (100%)	−1.07 (52.5%)	−0.97 (47.5%)	−0.3 (14.7%)	−0.67 (32.8%)
	0930	−2.01 (100%)	−0.47 (23.4%)	−1.54 (76.6%)	−0.3 (14.9%)	−1.24 (61.7%)
General budget§	**February**	**100%**	**4–28%**	**72–96%**	**4–27%**	**53–92%**
	September	**100%**	**9–52%**	**48–91%**	**6–25%**	**28–85%**

* Fauna-mediated O_2 uptake = total O_2 exchange − diffusive O_2 exchange.
† Fauna respiration calculated after mean species wet weight and empirical relations (Banta et al. 1999; Banse 1982).
‡ Burrow O_2 uptake = fauna-mediated O_2 uptake − fauna respiration.
§ Includes all determined flux rates from September and February.

that DOE is not controlled by the DBL thickness, while a ratio of <0.3 indicate a potential regulating effect of the DBL on the DOE. In our study $C_0:C_w$ was always >0.6 with an average of 0.78 ± 0.08 (SD, $n = 29$), and we therefore conclude that any DBL-related artifact was without importance for the DOE quantification in the present study. Another factor not included in the one-dimensional DOE calculations is the sediment topography (Jørgensen and Des Marais 1992; Røy et al. 2002). The one-dimensional flux approach does not account for the fact that the sediment area is larger than what is extrapolated from a flat plane and that the O_2 microsensor on the average penetrates the DBL at an angle (*see references above*). However, investigations taking the microtopograghy of the sediment surface into account using a three-dimensional measuring approach on typical coastal sediments revealed that the three-dimensional diffusive O_2 uptake on the average only was 13% higher than the traditional one-dimensional approach (Røy et al. 2002; Glud et al. 2003). We conclude that such effects were of minor importance in the present study.

O_2 mass balance of a coastal sediment—The DOE, the two-dimensional oxygen distribution, and the TOE allow us to establish a complete budget for the benthic O_2 consumption of the investigated sediment. The respiration of the enclosed *H. diversicolor* was calculated from the mean wet weight and empirical relations (Banse 1982; Banta et al. 1999) and was 0.3 and 0.2 mmol m^{-2} h^{-1} for September and February, respectively. These values represent an average value leading to an underestimation of faunal respiration during periods of enhanced activity and overestimation in resting periods. However, integrated over the entire night, the calculated fauna respiration only amounted to $<9\%$ and 12% of the TOE in September and February, respectively. The average O_2 uptake across the burrow wall can be calculated by subtracting the fauna respiration from the fauna-mediated O_2 uptake which, on the average, amounted to -0.75 mmol m^{-2} h^{-1} during daytime and -3.25 mmol m^{-2} h^{-1} at nighttime in September and -1.55 mmol m^{-2} h^{-1} at nighttime in February. It should be noted that the daytime calculation ignores any photosynthetic-related activity. As an example, different flux rates during the 24-h measuring cycle are presented in Table 1. These data show that, for all occasions, the fauna-mediated O_2 uptake was the dominant O_2 consumption process accounting for up to 92% of the total O_2 consumption. Laboratory experiments with the brittle star *Amphiura filiformis* revealed a similar value of 80% for the fauna-mediated O_2 uptake (Vopel et al. 2003). The O_2 uptake through the burrow wall, however, declined during night from 85% to 28% (Table 1) following the decreasing TOE (Fig. 4), which indicates that the fauna-stimulated consumption decreases during the night. We cannot exclude that the polychaetes actually were attracted to the periscope wall. Invertebrate fauna may prefer to establish themselves next to solid objects as they offer protection against predators and reduce burrow O_2 consumption. However, this does not change the conclusion based on the chamber and microprofile measurements or the fact that the community expressed a diel rhythm. But an accumulation of animals along the periscope wall could potentially exacerbate the observed O_2 dynamics of the surficial sediment.

From the integrated measurements performed in September and February, the major portion of the total benthic O_2 consumption was caused by fauna activity (48–96%). The majority of this was associated to O_2 respiration around burrow structures (53–93%) rather than to fauna respiration itself (7–49%). The relative contribution of each process, however, fluctuates with time, which was related to the varying levels of faunal activity. This again highlights the importance of fauna-stimulated O_2 consumption in coastal sediments, as opposed to faunal respiration or the diffusive uptake across the sediment surface.

Small-scale spatial and temporal variability—The two-dimensional oxygen distribution images provide further information of the small-scale O_2 consumption within the sed-

iment strata (Fig. 6). Local variations in the O_2 concentration within the sediment can be followed over time (Fig. 6A), and from extracted horizontal O_2 concentration profiles the oxygen banding around burrows can be estimated (Fig. 6B,C). The oxygen banding around animal burrows was estimated from a distinct break in the horizontal O_2 microprofile, which indicates the position of the burrow edges. In our study the oxygen banding varied between 1.1 and 5.9 mm with an average value of 2.7 ± 0.4 mm (SD, $n = 20$). However, the oxygen banding around the burrows varied strongly with time and environmental conditions, thus enhancing the complexity of procedures extracting information about the carbon mineralization form simple O_2 measurements. The oxygen banding of a single burrow, for example, increased from 0.4 to 0.8 mm between 0545 and 1000 h (Fig. 6B,C). Benthic primary production at the sediment surface, and in particular in the areas surrounding individual burrow openings, is the most likely explanation for the observed temporary extensions of the oxic regions. Oxygen-enriched bottom water was transported deep into the sediment enhancing the O_2 supply locally within the sediment and, thus, the O_2 penetration into the otherwise reduced sediment. In addition, enhanced faunal activity could have contributed to the O_2 availability in the burrow. Comparing the relative volume of oxygenated sediment below the sediment surface with that around burrows revealed that the major part (54–70%) was related to the burrow structures rather then to the sediment surface. Similar conclusions have previously been deduced from laboratory one-dimensional microsensor measurements (Fenchel 1996; Kristensen 2000).

By combining the O_2 penetration at the sediment surface and around burrows with the corresponding uptake rate (diffusive O_2 uptake or burrow O_2 uptake), the volume specific O_2 consumption rate was calculated. In our study the volume specific O_2 consumption in the oxygenated area around the burrows was in the range of 0.7–1 μmol cm^{-3} h^{-1} and grossly exceeded the equivalent rate at the sediment surface, which was in order of 0.03 to 0.10 μmol cm^{-3} h^{-1}. Burrow walls represent sites of enhanced mineralization (Aller and Aller 1986), and for *H. diversicolor* it has been shown that the mucus lining is enriched in labile organic carbon (Kristensen 2000). In our case, the major site for O_2 consumption was located around burrow structures, presumably as a result of intensified mineralization in the mucus layer and reoxidation of reduced compounds from the anaerobic degradation.

Synthesis and perspectives—We have shown that the O_2 consumption of coastal sediments is presumably more dynamic than previously anticipated. By integrating the presently available in situ technologies for quantifying the benthic O_2 dynamics we have established a budget of the O_2 consumption in a fauna-rich environment. Whereas microelectrodes provide a high-resolution insight in the O_2 dynamics of the DBL and at a single location within the sediment strata, the planar optode module reveals a detailed picture of the O_2 dynamics of the entire sediment profile. The two-dimensional images resolve the spatial and temporal variability of the O_2 distribution and provide crucial information on the fauna-stimulated consumption. The present fauna activity created a very dynamic O_2 distribution, which consequently affects the benthic mineralization. The extracted O_2 concentration profiles can, however, only be used to calculate fluxes and activities within the sediment. Owing to the wall effect of the inverted periscope, the DBL is distorted and simple DOE calculations on DBL based data are not meaningful (Glud et al. 1996).

The spatial and temporal effects of faunal activities on the sediment O_2 consumption, at a diel scale, are highly significant for any budget calculation. If this is a general phenomenon for coastal sediments, then this has a pronounced effect on the coastal carbon cycle.

References

ALLER, R. C. 1998. Benthic fauna and biogeochemical processes in marine sediments: The role of burrow structures, p. 301–338. *In* T. H. Blackburn and J. Sørensen [eds.], Nitrogen cycling in coastal marine environments. Wiley.

ALLER, J. Y., AND R. C. ALLER. 1986. Evidence for localized enhancement of biological activity associated with tube and burrow structures in deep-sea sediments at the HEBBLE site western North Atlantic. Deep-Sea Res. I **33:** 755–790.

ARCHER, D., AND A. DEVOL. 1992. Benthic oxygen fluxes on the Washington shelf and slope: A comparison of in situ microelectrode and chamber flux measurements. Limnol. Oceanogr. **37:** 614–629.

BANSE, K. 1982. Mass-scaled rates of respiration and intrinsic growth in very small invertebrates. Mar. Ecol. Prog. Ser. **9:** 281–297.

BANTA, G. T., M. HOLMER, M. H. JENSEN, AND E. KRISTENSEN. 1999. Effects of two polychaete worms, *Nereis diversicolor* and *Arenicola marina*, on a aerobic and anaerobic decomposition in a sandy marine sediment. Aquat. Microb. Ecol. **19:** 189–204.

BERG, P., N. RISGAARD-PETERSEN, AND S. RYSGAARD. 1998. Interpretations of measured concentration profiles in sediment porewater. Limnol. Oceanogr. **81:** 289–303.

CANFIELD, D., AND OTHERS. 1993. Pathways of organic carbon oxidation in three continental margin sediments. Mar. Geol. **113:** 27–40.

DEVOL, A. H., AND J. P. CHRISTENSEN. 1993. Benthic fluxes and nitrogen cycling in sediments of the continental margin of the eastern North Pacific. J. Mar. Res. **51:** 345–372.

EPPING, E. H. G., AND B. B. JØRGENSEN. 1996. Light enhanced oxygen respiration in benthic phototrophic communities. Mar. Ecol. Prog. Ser. **139:** 193–203.

FENCHEL, T. 1996. Worm burrows and oxic microniches in marine sediments. I. Spatial and temporal scales. Mar. Biol. **127:** 289–295.

———, AND R. N. GLUD. 2000. Benthic primary production and O_2-CO_2 dynamics in a shallow-water sediment: Spatial and temporal heterogeneity. Ophelia **53:** 159–171.

FORSTER, S., AND G. GRAF. 1995. Impact of irrigation on oxygen flux into the sediment: Intermittent pumping by *Callianassa subterranean* and 'piston-pumping' by *Lanice conchilega.* Mar. Biol. **123:** 335–346.

GLUD, R. N., AND N. BLACKBURN. 2002. The effect of chamber size on in situ benthic oxygen uptake measurements: A simulation study. Ophelia **56:** 23–31.

———, J. K. GUNDERSEN, AND N. B. RAMSING. 2000. Electrochemical and optical oxygen microsensors for in situ measurements, p. 19–72. *In* J. Buffle and G. Horvai [eds.], In situ

monitoring of aquatic systems: Chemical analysis and speciation. Wiley.

———, ———, N. P. REVSBECH, AND B. B JØRGENSEN. 1994. Effects on the diffusive boundary layer imposed by microelectrodes. Limnol. Oceanogr. **39:** 462–467.

———, ———, ———, ———, AND M. HUETTEL. 1995. Calibration and performance of the stirred flux chamber from the benthic lander Elinor. Deep-Sea Res. I **42:** 1029–1042.

———, ———, H. RØY, AND B. B. JØRGENSEN. 2003. Seasonal dynamics of benthic O_2 uptake in a semienclosed bay: Importance of diffusion and faunal activity. Limnol. Oceanogr. **48:** 1265–1276.

———, M. KÜHL, O. KOHLS, AND N. B. RAMSING. 1999. Heterogeneity of oxygen production and consumption in a photosynthetic microbial mat as studied by planar optodes. J. Phycol. **35:** 270–279.

———, ———, F. WENZHÖFER, AND S. RYSGAARD. 2002. Benthic diatoms of a high Artic fjord (Young Sound, NE Greenland): Importance for ecosystem primary production. Mar. Ecol. Prog. Ser. **238:** 15–29.

———, N. B. RAMSING, J. K. GUNDERSEN, AND I. KLIMANT. 1996. Planar optodes, a new tool for fine scale measurements of two-dimensional O_2 distribution in benthic communities. Mar. Ecol. Prog. Ser. **140:** 217–226.

———, A. TENGBERG, M. KÜHL, P. O. J. HALL, I. KLIMANT, AND G. HOLST. 2001. An in situ instrument for planar O_2 optode measurements at benthic interfaces. Limnol. Oceanogr. **46:** 2073–2080.

GUNDERSEN, J. K., AND B. B. JØRGENSEN. 1990. Microstructure of diffusive boundary layers and the oxygen uptake of the sea floor. Nature **345:** 604–607.

HARTMANN, P., W. ZIGLER, G. HOLST, AND D. W. LÜBBERS. 1997. Oxygen flux fluorescence lifetime imaging. Sensors Actuators B **38–39:** 110–115.

HOLST, G., O. KOHLS, I. KLIMANT, B. KÖNIG, M. KÜHL, AND T. RICHTER. 1998. A modular luminescence lifetime imaging system for mapping oxygen distribution in biological samples. Sensors Actuators B **74:** 78–90.

JØRGENSEN, B. B., AND B. P. BOUDREAU. 2001. Diagenesis and sediment-water exchange, p. 211–244. *In* B. P. Boudrau and B. B. Jørgensen [eds.], The benthic boundary layer: Transport processes and biogeochemistry. Oxford Univ. Press.

———, AND D. J. DES MARAIS. 1992. The diffusive boundary layer of sediments: Oxygen microgradients over a microbial mat. Limnol. Oceanogr. **35:** 1343–1355.

———, AND N. P. REVSBECH. 1985. Diffusive boundary layers and the oxygen uptake of sediments and detritus. Limnol. Oceanogr. **30:** 111–122.

KLIMANT, I., V. MEYER, AND M. KÜHL. 1995. Fiber-optic oxygen microsensor, a new tool in aquatic biology. Limnol. Oceanogr. **40:** 1159–1165.

KRISTENSEN, E. 2000. Organic matter diagenesis at the oxic/anoxic interface in coastal marine sediments, with emphasis on the role of burrowing animals. Hydrobiologia **426:** 1–24.

MCLACHLAN, A. 1983. Sandy beach ecology, p. 321–360. *In* A. McLachlan and T. Erasmus [eds.], Sandy beaches as ecosystems. Kluwer.

PIEPENBURG, D., AND OTHERS. 1995. Partitioning of benthic community respiration in the Arctic (northwestern Barents Sea). Mar. Ecol. Prog. Ser. **118:** 199–213.

PRECHT, E., U. FRANKE, L. POLERECKY, AND M. HUETTEL. 2004. Oxygen dynamics in permeable sediments with wave-driven pore water exchange. Limnol. Oceanogr. **49:** 693–705.

RASMUSSEN, H., AND B. B. JØRGENSEN. 1992. Microelectrode studies of seasonal oxygen uptake in a coastal sediment: Role of molecular diffusion. Mar. Ecol. Prog. Ser. **81:** 289–303.

REVSBECH, N. P. 1989. An oxygen microelectrode with a guard cathode. Limnol. Oceanogr. **34:** 474–478.

RHOADS, D. C., AND S. CANDE. 1971. Sediment profile camera for in situ study of organism-sediment relations. Limnol. Oceanogr. **16:** 110–114.

RIISGAARD, H. U., AND P. KAMERMANS. 2001. Switching between deposit and suspension feeding in coastal zoobenthos, p. 73–101. *In* K. Reise [ed.], Ecological comparisons of sedimentary shores. Springer.

ROSENBERG, R., AND L. LUNDBERG. In press. Photoperiodic activity pattern in the brittle star *Ampiura filiformis.* Mar. Biol.

RØY, H., M. HUETTEL, AND B. B. JØRGENSEN. 2002. The role of small-scale sediment topography for oxygen flux across the diffusive boundary layer. Limnol. Oceanogr. **47:** 837–847.

SMITH, JR., K. L., R. C. GLATTS, R. J. BALDWIN, S. E. BEAULIEU, A. H. UHLMAN, R. C. HORN, AND C. E. REIMERS. 1997. An autonomous, bottom-transecting vehicle for making long time-series measurements of sediment community oxygen consumption to abyssal depths. Limnol. Oceanogr. **42:** 1601–1612.

SOLAN, M., AND R. KENNEDY. 2002. Observation and quantification of in situ animal-sediment relations using time-lapse sediment profile imagery (t-SPI). Mar. Ecol. Prog. Ser. **228:** 179–191.

THAMDRUP, B., AND D. E. CANFIELD. 2000. Benthic respiration in aquatic sediments, p. 86–103. *In* O. E. R. Sala, R. B. Jackson, H. A. Mooney, and R. W. Horwarth [eds.], Methods in ecosystem science. Springer.

THERKILDSEN, M. S., AND B. A. LOMSTEIN. 1993. Seasonal variation in net benthic C-mineralization in a shallow estuary. FEMS Microbiol. Ecol. **12:** 131–142.

ULLMANN, W. J., AND R. C. ALLER. 1982. Diffusion coefficients in nearshore marine sediments. Limnol. Oceanogr. **27:** 552–556.

VOPEL, K., D. THISTLE, AND R. ROSENBERG. 2003. Effect of the brittle star *Amphiura filiformis* (Amphiuridae, Echinodermata) on oxygen flux into the sediment. Limnol. Oceanogr. **48:** 2034–2045.

WENZHÖFER, F., AND R. N. GLUD. 2002. Benthic carbon mineralization in the Atlantic: A synthesis based on in situ data from the last decade. Deep-Sea Res. I **49:** 1255–1279.

Received: 8 January 2004
Accepted: 16 May 2004
Amended: 27 April 2004